IEEE Access
Multidisciplinary : Rapid Review : Open Access Journal

Received 8 October 2023, accepted 19 October 2023, date of publication 23 October 2023, date of current version 30 October 2023.

Digital Object Identifier 10.1109/ACCESS.2023.3326727

RESEARCH ARTICLE

Probabilistic Bi-Level Assessment and Adaptive Control Mechanism for Two-Tank Interacting System

SAIBAL MANNA[1], **DEEPAK KUMAR SINGH**[2], **YAZEED YASIN GHADI**[3], **AMR YOUSEF**[4,5], **HOSSAM KOTB**[6], **AND KAREEM M. ABORAS**[6]

[1]Department of Electrical and Electronics Engineering, ABES Engineering College, Ghaziabad, Uttar Pradesh 201009, India
[2]Department of Electrical Engineering, National Institute of Technology, Jamshedpur, Jharkhand 831014, India
[3]Department of Computer Science and Software Engineering, Al Ain University, Abu Dhabi, United Arab Emirates
[4]Electrical Engineering Department, University of Business and Technology, Jeddah 23435, Saudi Arabia
[5]Engineering Mathematics Department, Faculty of Engineering, Alexandria University, Alexandria 21544, Egypt
[6]Electrical Engineering Department, Faculty of Engineering, Alexandria University, Alexandria 21544, Egypt

Corresponding author: Hossam Kotb (hossam.kotb@alexu.edu.eg)

ABSTRACT Liquid level control is a fundamental aspect employed across various industries, where the precise regulation of liquid levels and flow rates is of utmost importance. The Proportional-integral-derivative (PID)controller is widely employed but in practice, the operation of a PID may not always align with the desired outcome due to various factors such as system dynamic behavior, model uncertainties, time-varying parameters, and disturbances. To effectively address these challenges, the article proposes model reference adaptive control (MRAC) based on the Massachusetts Institute of technology (MIT) law feedback PID technique for a two-tank interacting system. The detailed comparative analysis is carried out in MATLAB/Simulink with open loop, PID, and MRAC in respect of time domain specifications. The proposed approach stability is verified using the Lyapunov approach. The robustness of the control mechanism is validated through probabilistic assessment by introducing a bi-level uncertainty framework such as gain mistuning and dynamic system behavior. In the first level, the gain mistuning is accomplished in three aspects i.e., fine-tuned, increased, and decrease gain. In the second level, it is considered that system behavior is dynamic in nature. Based on the findings, the MRAC-PID exhibits superior performance against uncertainties as compared to PID and MRAC with enhanced tracking rapidity, accuracy, and robustness.

INDEX TERMS Two-tank interacting system, PID, model reference adaptive controller (MRAC), MIT law, MRAC-PID.

I. INTRODUCTION

Raw materials, catalysts, intermediates, and end products are frequently fluidized in industrial chemical processes, necessitating a wide variety of storage vessels. In such instances, liquids are stored in one tank and then transferred in a controlled way to another tank. It is widely acknowledged that tanks and the mechanisms used to regulate their levels and flows form the backbone of every chemical engineering system [1]. Therefore, effectively controlling of these parameters in the process industries also demonstrates significant economic advantages. Liquid level control is simpler to measure and observe when compared to other variables like pressure, flow rate, and other parameters. Hence, it is crucial to closely observe and track the fluid level inside a manufacturing operation. The system's operational status may be accurately determined by observing whether it operates within its critical limits or is experiencing a malfunction. Disqualified products and accidents may result from an irregular liquid level in the manufacturing process [2].

Liquid level control has several uses in industry, including in the nuclear power industry, the chemical and food industries, the paper industry, the coating and water treatment industries, and many more. The liquid level system

The associate editor coordinating the review of this manuscript and approving it for publication was Zheng Chen.

operates in accordance with the principles of hydromechanics and exhibits typical nonlinearity, large time delay, strong coupling, great inertia, and constrained multivariable [3]. A precise level of control plays a crucial role in these processes from an economic standpoint. Various control approaches, including proportional integral differential (PID) control [4], [5], fuzzy control [6], [7], [8], backstepping approach [9], sliding mode control (SMC) [10], [11], [12], and fractional order technique [13], [14] have been employed to speed up the attainment of desirable equilibrium points and sustain the system's stability.

It is widely acknowledged that numerous processes can be effectively regulated by employing PI or PID controllers. The tuning methods commonly employed in industrial applications encompass the Ziegler-Nichols and Cohen-Coon techniques [15]. These techniques assume that the system is linear w.r.t the operational point. To maintain the operational point under this circumstance, we derive adjustable values of the integral gain (K_I), derivative gain (K_D), and proportional gain (K_P). When process dynamics are slow, it might be challenging to fine-tune a PID controller with three adjustable parameters [10].

In the event of alterations in operating conditions, it becomes necessary to readjust the parameters of the PID controller. Therefore, in these methodologies, it necessitates the involvement of a human operator. The unanticipated variation in process parameters detrimentally impacts the desired operational characteristics of the system in real-time. Hence, the efficacy of a PID controller may not consistently correspond with the desired response due to various uncertainties [16], [17].

Using a hybrid chaotic Henry gas solubility optimization and feedback artificial tree i.e., CHGSO-FAT approach, the level control of liquid in a two-tank interacting spherical system with fractional order PID (FOPID) is suggested. A spherical two-tank system's liquid level can be properly regulated using the suggested controller. The CHGSO-FAT controller has advantages over PI, PID, and PID-Sliding mode control (SMC) in that it significantly minimizes undershoot and overshoot, reduces peak, rise, and settling time, and also provides low ISE and IAE. Nevertheless, the proposed approach is complex and takes much time to follow the set point [18]. The fuzzy FOPID technique is suggested to manage the level control of liquid in a two-tank interacting spherical system. The suggested control scheme's indices for instance overshoot, peak, rise, and settling time are compared to PID-SMC, FOPID, PI, and PID. The suggested scheme's external disturbance rejection capacity is proven for step inputs. The experimental prototype findings demonstrate the controller's efficacy. However, the robustness of the suggested method has not been proven in the presence of model uncertainty and mistuning of controller parameters [19].

This study compares and assesses gap metric-based weighting approaches to the construction of multimodal control mechanisms for level regulation in conical and spherical tank processes through experimental setup. The corresponding linear models are created for the internal mode control-PI technique. The study of level regulation in conical and spherical tank setups demonstrates the successful experimental application of the multi-model control strategies under consideration [20]. An observer controller strategy for a state-coupled two-tank setup is presented in the research. The usefulness of the suggested sensor less control strategy in terms of observation, quick transient reaction, and high tracking accuracy is highlighted by both experiment and simulation results [21]. The authors discussed liquid level regulation using the FOPID method in a three-tank system. Compared to the PID controller, the suggested FOPID offers enhanced process performance development [22]. To control the level of nuclear power plant's steam generators, a hybrid SMC strategy was described in this study. The suggested method stabilizes the system in the face of disturbances and reference changes; in each test run, the system reaction shows negligible overshoot and slowly rises to the required water level. For disturbance rejection and set-point tracing, the performance obtained with the suggested strategy was suitable [23]. This paper applies the SMC based upon linear extended state observer (SMC-LESO) to the problem of controlling the water level in a drum, thereby combining the benefits of the two approaches. Simulation findings demonstrate the SMC-LESO's strengths, including low overshoot, fast settling time, potent anti-interference capability, and high resilience [24].

A new architecture is presented for the integration of IoT technology in order to enable intelligent monitoring and management of flow rate and pressure inside a fluid transportation system. It employs SCADA with LQR-PID as a local control unit. The integrated IoT architecture is verified experimentally in lab and provides better performance compared to Zigler-Nichols and Internal-Mode controller. However, the performance of the set point tracking is not very remarkable, as the model uncertainty was not taken into consideration [25]. Due to the inherent fluid nature of molten salt fuel within a liquid molten salt reactor, the development of a precise mathematical model for the core power control system is a significant challenge. A fuzzy-PID composite control approach is proposed as a solution to address the problem. The error range determines whether the composite controller uses PID or fuzzy technique to control the system. Nevertheless, the controller's resilience has not been evaluated in the presence of model uncertainty and parameter mistuning [17].

An interval type-2 fuzzy FOPID controller is introduced to address the load reduction scenario in pumped storage units operating with small loads and low water head. In order to fine-tune controller parameters, a multi-objective joint optimization technique is presented. After optimizing the parameters, the experimental findings demonstrate that the proposed controller outperforms conventional controllers. However, the proposed technique is complex [26]. For the purpose of controlling the water level in a two-tank hybrid system, a SMC is designed with sliding surface based on

FOPID technique. An enhanced SMC approach is presented, incorporating a FOPID sliding surface in which the system's output is directly used as the input for the derivative component in the sliding surface equation. Based on simulation results, the suggested SMC with FOPID sliding surface outperforms the traditional SMC, SMC-FOPID and SMC-FOPD sliding surface. Furthermore, the performance of set point tracking is not very remarkable, and it has not been subjected to testing for the resilience of the controller in the presence of model uncertainty [27]. For the purpose of water level control of the nuclear steam generator, a gain-scheduled equivalent-cascade internal-model-control (IMC) tuning approach is introduced. The experimental findings of the nuclear simulation platform have provided evidence for the effectiveness of the suggested tuning procedure [28].

A Dynamic SMC (DSMC) is introduced, which is developed by using the Iinoya and Altpeter technique and SMC design process. The suggested method is applied for high-order chemical processes that have inverse response and long dead time. The experimental findings reveal that the tracking, control, and parameter uncertainties of the proposed DSMC are remarkably similar to the SMC [29]. An adaptive fuzzy cooperative control based on sliding surface is introduced for multi-electromagnet suspension systems of low and medium-speed maglev trains. The superior performance of the devised approach is demonstrated experimentally by comparing it to certain baseline methods such as PID and Fuzzy PID, and the results of the suspension frame experiments are presented to confirm the efficacy and resilience of the method [30]. An adaptive control strategy based on neural networks is developed to maintain a constant airgap for a nonlinear maglev train. In order to address the issue of uncertainty, the basic controller is enhanced by including a radial basis function neural network. This integration enables a more efficient and precise recovery of the unknown mass and disturbance [31]. An intelligent neuro-controller based on an artificial neural network (ANN) is proposed for a nonlinear process tank system. In this case, the Levenberg-Marquardt method was used to train the network. Comparative results show the suggested model performs better in terms of undershoot, settling time, and overshoot in MATLAB platform [1]. An adaptive disturbance attenuation control approach based on the port-controlled Hamiltonian model is introduced to examine the problems associated with the two-tank liquid level system. The efficacy and resilience of the proposed control algorithm are demonstrated through the simulation and experimental findings [3].

As per the literature survey, it is analyzed that the probabilistic bi-level performance assessment of the control mechanism is not carried out by any researchers for the two-tank interacting system. Meanwhile, the dynamic and static performance of the considered system is not so impressive. This motivates the authors to design an adaptive control mechanism such that it quickly adapts the uncertainties and gives better system performance. This research paper presents the development of a model reference adaptive control-proportional integral derivative (MRAC-PID) controller for a two-tank interaction system and the stability of the closed-loop system is then investigated using the Lyapunov stability approach. The important efforts are listed here:

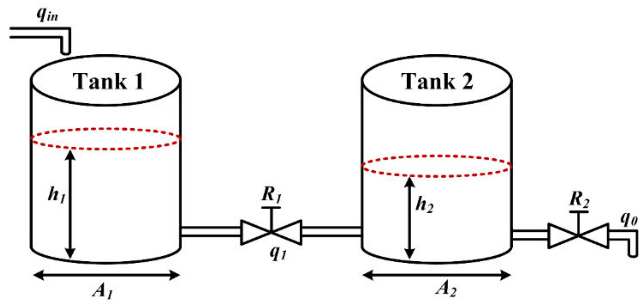

FIGURE 1. Two-tank interacting system.

1. Design and development of novel MRAC-PID control mechanism for the two-tank interacting cylindrical system.
2. The conventional MRAC is structured for the first-order system. However, the majority of the plants are second-order systems including two-tank interacting systems. Since the conventional MRAC performance is not up to the mark. Therefore, MRAC's first to second-order extension is developed and the control law is implemented for the second-order system.
3. The response of the proposed MRAC-PID and conventional MRAC are comparatively analyzed considering different adaptive gains and parameters for a two-tank interacting system.
4. The probabilistic assessment is accomplished through a bi-level uncertainty framework such as Level I: Gain mistuning; Level II: Dynamic system behavior.
5. The performances of the proposed MRAC-PID control mechanism are vividly compared with PID and conventional MRAC technique in terms of time domain specifications (overshoot, rise time, settling time, and peak time) and error indices (ISE, IAE, and ITAE).

This paper will have the following structure. Next, section II looks at how this particular two-tank coupled system can be modeled dynamically. The construction of both the conventional and suggested MRAC control mechanism for a two-tank setup is addressed in Section III. The stability analysis of the proposed controller is discussed in Section IV. Section V presents simulation findings, as well as comparisons with well-known techniques, to validate the utility of the proposed adaptive control mechanism. In Section VI, conclusions are incorporated.

II. SYSTEM DESCRIPTION AND MATHEMATICAL MODELING

Figure 1 depicts the two-tank interacting system. Tank 1 and 2 receive flow rates of q_{in} (cm^3/min) and q_1 (cm^3/min)

TABLE 1. Cylindrical tank specifications [32].

Symbol	Description	Value
R_1	Resistance	1.5 Ω
R_2	Resistance	1.7 Ω
D	Diameter of tank	92 cm
q_{in}	Initial flow	20 lph
τ_1	Time constant	0.9
τ_2	Time constant	1.02

respectively, while tank 2 releases through a flow rate of $\boldsymbol{q_0}$ (cm^3/min). Now, $\boldsymbol{h_1}$ and $\boldsymbol{h_2}$ in mm is the liquid level height in tanks 1 and 2 correspondingly, and the cross-sectional area of both tanks is similar. Next, tanks 1 and 2 have areas of $\boldsymbol{A_1}$ (cm^2) & $\boldsymbol{A_2}$ (cm^2) respectively. Tank 1 & 2 have an inflow rate of $\boldsymbol{q_{l1}}$ and $\boldsymbol{q_{l2}}$ in (cm^3/min) as load disturbance. Tank 1 and 2 differential equations are presented in equations (1) and (8) respectively.

The mass balance formula for tank 1 is described as,

$$A_1\frac{dh_1}{dt} = q_{in} - q_1 \tag{1}$$

Consider linear resistance flow,

$$q_1 = \frac{h_1 - h_2}{R_1} \tag{2}$$

$$A_1\frac{dh_1}{dt} = q_{in} - \frac{h_1 - h_2}{R_1} \tag{3}$$

$$A_1R_1\frac{dh_1}{dt} = q_{in}R_1 - h_1 + h_2 \tag{4}$$

By taking Laplace's transform

$$A_1R_1sh_1(s) = q_{in}(s)R_1 - h_1(s) + h_2(s) \tag{5}$$

$$h_1(s) = \frac{R_1q_{in}(s) + h_2(s)}{1 + A_1R_1s} \tag{6}$$

$$h_1(s) = \frac{R_1q_{in}(s) + h_2(s)}{1 + \tau_1 s} \tag{7}$$

where $\tau_1 = A_1R_1$. Similarly, the mass balance equation for tank 2 is expressed as

$$A_2\frac{dh_2}{dt} = q_1 - q_0 \tag{8}$$

Again, consider linear resistance flow,

$$A_2\frac{dh_2}{dt} = \left(\frac{h_1 - h_2}{R_1}\right) - \left(\frac{h_2}{R_2}\right) \tag{9}$$

where $q_0 = \frac{h_2}{R_2}$

$$A_2R_1R_2\frac{dh_2}{dt} = R_2h_1 - R_2h_2 - h_2R_1 \tag{10}$$

On dividing by R_1 and taking Laplace transform,

$$A_2R_2sh_2(s) + \frac{R_2}{R_1}h_2(s) + h_2(s) = \frac{R_2}{R_1}h_1(s) \tag{11}$$

$$h_2(s)\left(\tau_2 s + \frac{R_2}{R_1} + 1\right) = \frac{R_2}{R_1}h_1(s) \tag{12}$$

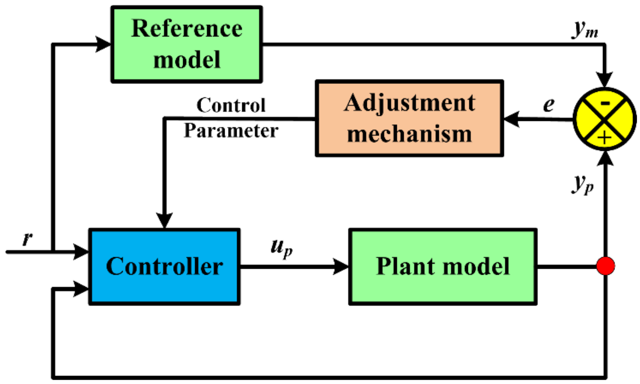

FIGURE 2. Conventional MRAC block diagram.

where $\tau_2 = A_2R_2$ and put the value of $h_1(s)$ from equation (7), we get

$$h_2(s)\left(\tau_2 s + \frac{R_2}{R_1} + 1\right) = \frac{R_2}{R_1}\left(\frac{R_1q_{in}(s) + h_2(s)}{1 + \tau_1 s}\right) \tag{13}$$

$$h_2(s)\left(\tau_2 s + \tau_2\tau_1 s^2 + \frac{R_2}{R_1}\tau_1 s + 1 + \tau_1 s\right) = R_2q_{in}(s) \tag{14}$$

Hence, for the two-tank interacting system, the transfer function is obtained as

$$\frac{h_2(s)}{q_{in}(s)} = \frac{R_2}{\tau_2\tau_1 s^2 + (\tau_1+\tau_2 + A_1R_2)s + 1} \tag{15}$$

Solving equation (15) with the parameters listed in Table 1 yields the transfer function of the system under consideration.

$$G(s) = \frac{1.7}{0.918s^2 + 1.935s + 1} \tag{16}$$

III. CONTROLLER DESIGN MECHANISM

A. MODEL REFERENCE ADAPTIVE CONTROLLER (MRAC)

The response of a system utilizing a regular feedback loop becomes erroneous when the parameters are not precisely recognized, and adaptive control is then employed.

In MRAC, a reference model defines the expected behavior of the process, and the controller parameters are changed depending on error (e), which is determined as the discrepancy between the process outcome (y_p) and the output of the reference model (y_m). As illustrated in Figure 2, MRAC has two loops: an outer loop (or adaptation) that modifies the controller's variable in order to reduce the error between the reference and plant model output to zero, and an inner loop that functions as a simple control loop between plant and controller.

The primary elements of the MRAC are the reference model, controller, and adaptation mechanism.

Reference model: The purpose of this model is to define the desired behavior of the adaptive control in response to exterior commands. The design must accurately embody the operation stipulation required for the control mechanism. The desired performance characteristics outlined by the reference model should be attainable within the adaptive control system. The reference model for this study is the critically damped second-order system.

Controller: The controller design typically involves the parameterization of a set of adjustable parameters (θ_1, θ_2 and θ_3). The control law exhibits linearity w.r.t the adjustable parameters, adhering to a linear parameterization. In the realm of adaptive controller design, it is customary to employ linear parameterization to achieve an adaptation mechanism that ensures both convergence in tracking and stability. The control parameters' values are primarily influenced by the adaptation gain, which subsequently modifies the control strategy of the adaptation mechanism.

Adaptation mechanism: The purpose of this mechanism is to facilitate the manipulation of parameters within the control rule. The adaptation rule seeks to identify optimal parameters, ensuring that the plant's response aligns with the desired behavior specified by the reference model. The design guarantees the control system stability while also achieving convergence of the error tracking to zero. In the realm of controller design engineering, various mathematical techniques such as Lyapunov theory, MIT rule, and augmented error concept can be effectively employed to formulate and refine the adaptation mechanism. In such a considered system, the MIT rule is employed for this specific purpose.

The input and output signal of the plant is denoted by $u_p(t)$ and $y_p\,(t)$ respectively. The following form, appropriate in both frequency and time domains, was chosen as the second-order plant model.

$$\frac{d^2y_p(t)}{dt^2} = -a_p\frac{dy_p\,(t)}{dt} - b_py_p\,(t) + k_pu_p(t) \tag{17}$$

$$G_p(s) = \frac{y_p(s)}{u_p(s)} = \frac{k_p}{s^2 + a_ps + b_p} \tag{18}$$

where a_p, b_p and k_p are plant parameters and they can be determined using equation (16). The following form describes the relation between the input $r(t)$ and the intended output $y_m\,(t)$ in the second-order reference model (in both the time and frequency domains).

$$\frac{d^2y_m(t)}{dt^2} = -a_m\frac{dy_m\,(t)}{dt} - b_my_m\,(t) + k_mr(t) \tag{19}$$

$$G_m(s) = \frac{y_m(s)}{r(s)} = \frac{k_m}{s^2 + a_ms + b_m} \tag{20}$$

where k_m represents positive gain, and b_m and a_m are chosen as the response of the reference model is critically damped. The goal of the control strategy is to develop $u_p(t)$ so that plant output $y_p\,(t)$ follows reference model output $y_m\,(t)$ asymptotically. The parameters of the MRAC controller's adaption law are calculated using the MIT rule. As per MIT law, the cost function is formulated as:

$$J(\theta) = \frac{e^2}{2} \tag{21}$$

$$e = y_p - y_m \tag{22}$$

The difference between plant and reference model i.e., $(y_p - y_m)$ constitutes the error which is denoted by e. The control parameter that can be adjusted is represented by the symbol θ. To achieve the goal of reducing the overall cost function to its minimum possible, the value of the θ is adjusted using the MIT rule, which is given in equation (21). As a result, it is written.

$$\frac{d\theta}{dt} = -\lambda\frac{\delta J}{\delta\theta} = -\lambda e\frac{\delta e}{\delta\theta} \tag{23}$$

where the terms λ and $\frac{\delta e}{\delta\theta}$ are used to describe adaptation gain and sensitivity derivative, respectively. The controller architecture for accomplishing the targeted control goals is depicted in Figure 3. The control law $u_p(t)$ is defined for bounded reference input.

$$u_p = \theta_1 r - \theta_2 y_p - \theta_3\dot{y}_p = \theta^T\varphi \tag{24}$$

where the estimated vector of the controller parameter is denoted by $\theta = [\theta_1, \theta_2, \theta_3]^T$ and φ presents $\left[r, y_p, \dot{y}_p\right]^T$. Substituting equation (24) into equation (17), we get

$$\frac{d^2y_p(t)}{dt^2} = -\left(a_p + k_p\theta_3\right)\frac{dy_p\,(t)}{dt} - \left(b_p + k_p\theta_2\right)y_p\,(t) + k_p\theta_1r(t) \tag{25}$$

Comparing equations (19) and (25) coefficients, we get

$$k_m = \theta_1k_p \tag{26}$$

$$b_m = b_p + k_p\theta_2 \tag{27}$$

$$a_m = a_p + k_p\theta_3 \tag{28}$$

where θ_1, θ_2, and θ_3 are control parameters and they are converged as:

$$\theta_1 \approx \frac{k_m}{k_p};\ \theta_2 \approx \frac{b_m - b_p}{k_p};\ \theta_3 \approx \frac{a_m - a_p}{k_p} \tag{29}$$

Taking the Laplace transform of the equation (25), we get

$$\frac{y_p(s)}{r(s)} = \frac{k_p\theta_1}{s^2 + \left(a_p + k_p\theta_3\right)s + \left(b_p + k_p\theta_2\right)} \tag{30}$$

As per the error equation (22), we can write

$$e = \left(\frac{k_p\theta_1}{s^2 + \left(a_p + k_p\theta_3\right)s + \left(b_p + k_p\theta_2\right)} - \frac{k_m}{s^2 + a_ms + b_m}\right)r(s) \tag{31}$$

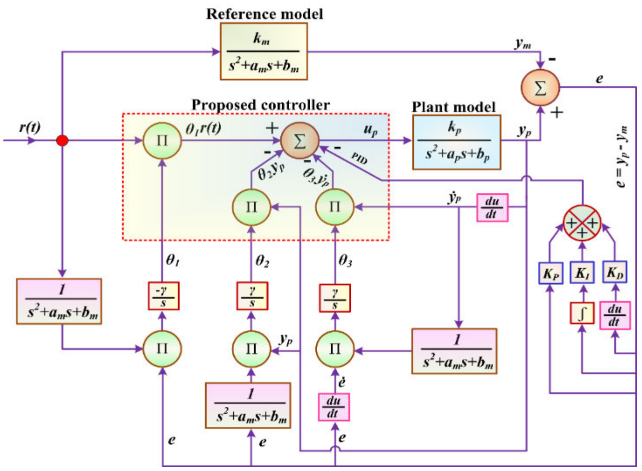

FIGURE 3. Inner architecture of proposed MRAC-PID control mechanism.

The sensitivity derivatives $\frac{\delta e}{\delta \theta_1}$, $\frac{\delta e}{\delta \theta_2}$ and $\frac{\delta e}{\delta \theta_3}$ are derived from equations (30) & (31) given by

$$\frac{\delta e}{\delta \theta_1} = \frac{k_p r}{s^2 + a_p s + k_p \theta_3 s + b_p + k_p \theta_2} \tag{32}$$

$$\frac{\delta e}{\delta \theta_2} = \frac{-k_p y_p}{s^2 + a_p s + k_p \theta_3 s + b_p + k_p \theta_2} \tag{33}$$

$$\frac{\delta e}{\delta \theta_3} = \frac{-k_p y_p s}{s^2 + a_p s + k_p \theta_3 s + b_p + k_p \theta_2} \tag{34}$$

Considering $s^2 + a_m s + b_m = s^2 + a_p s + k_p \theta_3 s + k_p \theta_2 + b_p$. In equation 23, the $\frac{\delta e}{\delta \theta}$ are replaced following the MIT rule (equations 21 and 23). After restructuring, the equations (35), (36), and (37) are employed to modify control parameters θ_1, θ_2, and θ_3 respectively.

$$\frac{d\theta_1(t)}{dt} = -\lambda \left(\frac{1}{s^2 + a_m s + b_m} r(t) \right) e(t) \tag{35}$$

$$\frac{d\theta_2(t)}{dt} = \lambda \left(\frac{1}{s^2 + a_m s + b_m} y_p(t) \right) e(t) \tag{36}$$

$$\frac{d\theta_3(t)}{dt} = \lambda \left(\frac{1}{s^2 + a_m s + b_m} \dot{y}_p(t) \right) \dot{e}(t) \tag{37}$$

The MRAC controller design has been finalized, and the proposed control mechanism is described in the subsequent section.

B. PROPOSED MRAC-PID CONTROL MECHANISM

The response of the reference model is utilized for monitoring the outcome of the plant through MRAC. The required outcomes will certainly be realized by establishing the reference model. However, using solely conventional MRAC is insufficient to boost system performance. Consequently, a modified version of the MRAC i.e., MRAC-PID control mechanism, is developed. The internal architecture of the proposed MRAC-PID control mechanism is depicted in Figure 3.

The PID provides feedback for MRAC and the performance of the system is significantly enhanced as MRAC-PID controller is combined. It should be noted that the proposed controller's (MRAC-PID) output depends not only on the adaption gain but also on the proportional (K_P), integral (K_I) and derivative (K_D) gains of the PID block. The control law is expressed as:

$$u_p = \theta_1 r - \theta_2 y_p - \theta_3 \dot{y}_p - \left(K_P e + K_I \int e dt + K_D \frac{de}{dt} \right) \tag{38}$$

In comparison to traditional MRAC, the combined effect of MRAC and PID feedback, or MRAC-PID, on the second-order two-tank interacting system leads to enhanced process behavior during transient as well as steady-state responses. The control rule is employed to align the response of the plant and standard model, and it is given in equation (39).

$$G_m(s) = \frac{50}{s^2 + 15s + 50} \tag{39}$$

IV. STABILITY ANALYSIS

Lyapunov theory is used to analysis the stability of the system. To minimize the error, it makes sense to formulate it as a differential equation. The error equation in (22), when its first and second derivatives are taken, looks like this:

$$\frac{de}{dt} = \frac{dy}{dt} - \frac{dy_m}{dt} \tag{40}$$

$$\frac{d^2e}{dt^2} = \frac{d^2y}{dt^2} - \frac{d^2y_m}{dt^2} \tag{41}$$

When equations (17) and (19) are substituted into equation (41), and u_p is substituted as in (24), we get:

$$\frac{d^2e}{dt^2} = \frac{dy_p}{dt}\left(-a_p - k_p\theta_3 + a_m\right) + y_p\left(-b_p - k_p\theta_2 + b_m\right) + r\left(k_p\theta_1 - k_m\right) - a_m\frac{de}{dt} - b_m e \tag{42}$$

If the values of the parameters are the same as those in equation (29), then $e(t)$ is zero. According to Lyapunov's stability theorem, a system is asymptotically stable if there is a scalar function $V(t)$ that is real, continuous, and has continuous first partial derivatives with $\dot{V}(t) < 0$ for all $t \neq 0$,

Assume $k_p\lambda > 0$ and define the Lyapunov function V as:

$$V(e, \dot{e}, \theta_1, \theta_2, \theta_3) = \frac{1}{2}\frac{(a_p + k_p\theta_3 - a_m)^2}{k_p\lambda} + \frac{1}{2}\frac{(b_p + k_p\theta_2 - b_m)^2}{k_p\lambda} + \frac{1}{2}\frac{(k_p\theta_1 - k_m)^2}{k_p\lambda} + \frac{1}{2}\left(\frac{de}{dt}\right)^2 + \frac{1}{2}b_m e^2 \tag{43}$$

For this function, $V=0$ when $e=0$, and the controller parameters are equal to the correct values. When $\frac{dV}{dt}$ is negative, the

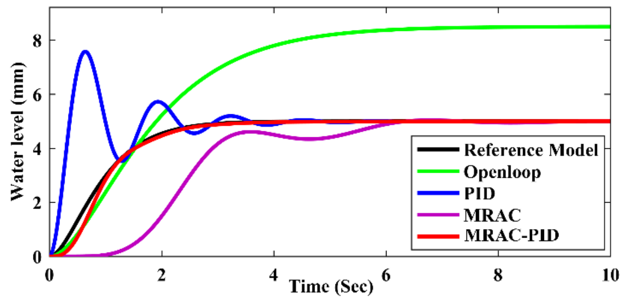

FIGURE 4. Output response of the two interacting couple tank systems using the open loop, PID, MRAC, and MRAC-PID (λ =0.08).

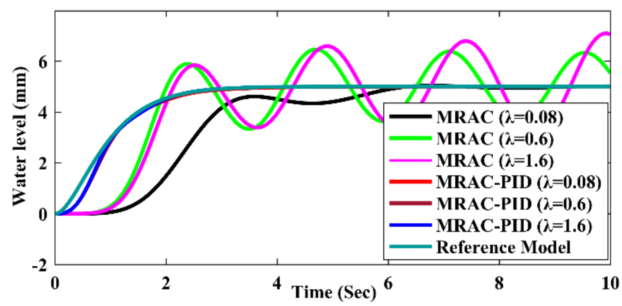

FIGURE 5. Output response of the two interacting couple tank systems using MRAC, and MRAC-PID under different adaptation gains.

function is a Lyapunov one. The derivative is given as:

$$\frac{dV}{dt} = \frac{(a_p + k_p\theta_3 - a_m)}{\lambda}\left(\frac{d\theta_3}{dt} - \dot{e}\dot{y}_p\right) + \frac{(b_p + k_p\theta_2 - b_m)}{\lambda}\left(\frac{d\theta_2}{dt} - \dot{e}y_p\right) + \frac{(k_p\theta_1 - k_m)}{\lambda}\left(\frac{d\theta_1}{dt} + \dot{e}r\right) - a_m\dot{e}^2 \quad (44)$$

If the parameters are updated as $\dot{\theta_1} = -\gamma r\dot{e}$, $\dot{\theta_2} = \gamma y_p\dot{e}$ and $\dot{\theta_3} = \gamma\ \dot{y}_p\dot{e}$. There is:

$$\frac{dV}{dt} = -a_m\dot{e}^2 \quad (45)$$

Thus, the time derivative of V is negative semidefinite rather than negative definite. Therefore, it implies $V(t) \leq V(0)$ and thus, θ_1, e,θ_2, $\dot{e}$, andθ_3 must be bounded. This concludes that $y_p = e + y_m$ is also bounded. Now a necessary condition to prove is $\ddot{V}$ bounded. $\ddot{V}$ is given as:

$$\frac{d^2V}{dt^2} = -2a_m\dot{e}\frac{d\dot{e}}{dt} = -2a_m\dot{e}\begin{cases} -\dfrac{dy_p}{dt}\left(a_p + k_p\theta_3 - a_m\right) \\ -y_p\left(b_p + k_p\theta_2 - b_m\right) \\ +r\left(k_p\theta_1 - k_m\right) \\ -a_m\dfrac{de}{dt} - b_m e \end{cases} \quad (46)$$

Since r, e,and y_p are bounded, it follows that $\ddot{V}$ is also bounded. Hence, $\frac{dV}{dt}$ is uniformly continuous.

V. RESULTS AND ANALYSIS

The MRAC-PID controller is designed using the MATLAB/ Simulink platform, and compared to well-known techniques such as PID and conventional MRAC. The plant model is described in Equation 16 and its specifications are given in Table 1. The different error indices are calculated using the following equations [33].

$$Integral\ absolute\ error\ (IAE) = \int_0^\infty |e(t)|\,dt \quad (47)$$

$$Integral\ square\ error\ (ISE) = \int_0^\infty |e(t)|^2\,dt \quad (48)$$

$$Integral\ time\ absolute\ error\ (ITAE) = \int_0^\infty t\,|e(t)|\,dt \quad (49)$$

Directly providing input to the system and examining its characteristics is known as the open loop response of a system. The output of an open loop control is not evaluated or provided for signal compared to the input. In a closed-loop system, a controller is employed to perform a comparison between the system's response and the desired condition, subsequently transforming the error into a control action. It is built to minimize error and enable the system for attaining the desired outcome.

The fine-tuned PID controller gains are such as $K_P = 13$, $K_I = 5$ and $K_D = 0.1$, and the adaption gain (λ) is determined as 0.08. The output response of the two interacting coupled tank systems using the open loop, PID, MRAC, and proposed MRAC-PID is displayed in Figure 4. It is evident that PID takes 6.07 Sec, conventional MRAC takes 6.26 Sec and the proposed MRAC-PID requires only 3.30 Sec to track the desired outcome. The PID controller has a higher overshoot whereas the MRAC and proposed control mechanism have negligible overshoot.

A. SIMULATION WITH DIFFERENT ADAPTIVE GAINS AND PARAMETERS

The MRAC component that directly impacts system functionality is the adaptation gain (λ). It shouldn't be either too high or low. One of the user-defined variables in the adaptive control law is the λ [34].

For the MRAC, three adaptation gains are determined such as $\lambda = 0.08$, 0.6, and 1.6. The optimum value of PID gains is also used in this case. The response of the MRAC and MRAC-PID for different values of λ is depicted in Figure 5.

Table 2 incorporates the set point tracing of the control mechanism for different adaption gains. At $\lambda = 0.08$, the settling duration, overshoot, and rise time for the PID, MRAC, and MRAC-PID are 6.07 Sec, 53.077%, and 0.247 Sec; 6.26 Sec, 0%, and 1.747 Sec; & 3.30 Sec, negligible, and 1.614 Sec respectively.

Table 3 encompasses the error indices of the control mechanism for different adaption gains. At $\lambda = 0.08$, the error such as IAE, ISE, and ITAE for the PID, MRAC, and MRAC-PID are 0.001955, 3.821×10^{-6}, and 0.01955; 0.0002056, 0.04134, and 0.1434; & 0.0008052, 6.484×10^{-7}, and 0.008052 respectively. Upon a careful investigation of all

TABLE 2. Set point tracing at different adaptation gains.

Control mechanism	Adaptation gain (λ)	Set point tracing		
		Settling time (Sec)	Overshoot (%)	Rise time (Sec)
PID	-	6.07	53.077	0.247
MRAC	0.08	6.26	0	1.747
	0.6	Fluctuating	11.798	0.805
	1.6	Fluctuating	19.676	0.861
MRAC-PID	0.08	3.30	0	1.614
	0.6	3.41	0	1.600
	1.6	3.38	0	1.560

TABLE 3. Error indices at different adaptation gains.

Control mechanism	Adaptation gain (λ)	Error indices		
		IAE	ISE	ITAE
PID	-	0.001955	3.821×10^{-6}	0.01955
MRAC	0.08	0.0002056	0.04134	0.1434
	0.6	0.5271	0.2779	5.271
	1.6	2.053	4.213	20.53
MRAC-PID	0.08	0.0008052	6.484×10^{-7}	0.008052
	0.6	6.086×10^{-6}	3.704×10^{-11}	6.086×10^{-05}
	1.6	3.372×10^{-6}	1.137×10^{-11}	3.372×10^{-5}

TABLE 4. Comparative analysis with different adaptive gains and parameters.

Control mechanism	Adaptation gain (λ)	Adaptive parameters		
		θ_1	θ_2	θ_3
MRAC	0.08	2.32	-0.6	-0.08
	0.6	2.8 to 4.8	0.25 to -1.25	0.15 to -0.2
	1.6	2.4 to 4.2	0.48 to -1.5	0.2 to -0.2
MRAC-PID	0.08	0.05	-0.05	0.05
	0.6	0.52	-0.15	0.38
	1.6	1.15	-0.2	1

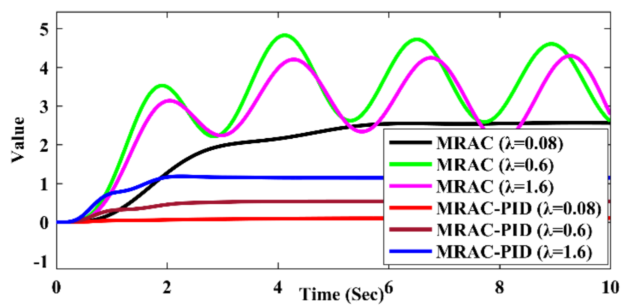

FIGURE 6. Change of adaptive parameter (θ_1) at different adaptation gains.

conditions, it is evident that the utilization of $\lambda = 0.08$ results in a notable improvement in the overall operational efficacy and dynamic performance of the MRAC-PID control mechanism for the two-tank interacting system.

The change of adaptive parameters such as θ_1, $\theta_2$andθ_3 of the MRAC and MRAC-PID at different adaptation gains ($\lambda = 0.08, 0.6, 1.6$) are depicted in Figures 6, 7, and 8 respectively.

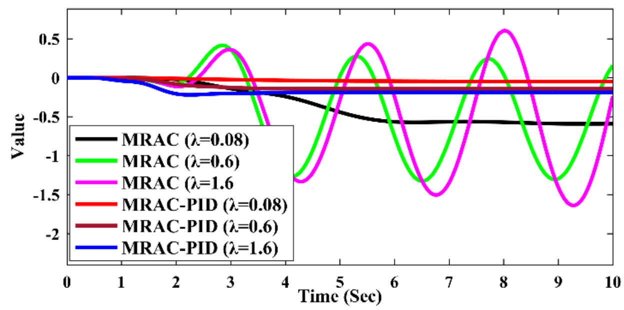

FIGURE 7. Change of adaptive parameter (θ_2) at different adaptation gains.

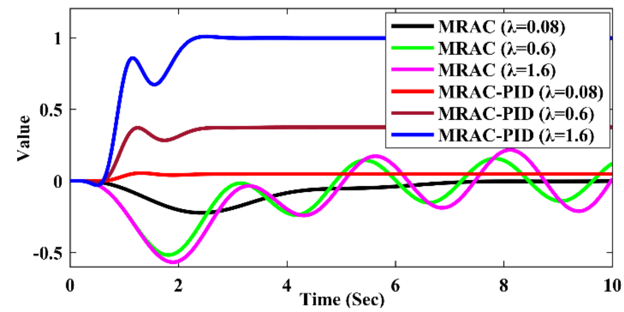

FIGURE 8. Change of adaptive parameter (θ_3) at different adaptation gains.

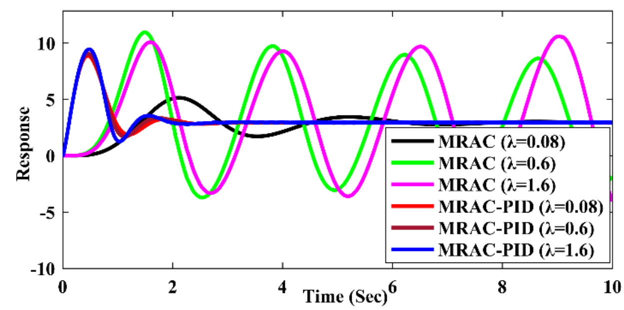

FIGURE 9. Control performance of MRAC and MRAC-PID under different adaptation gains.

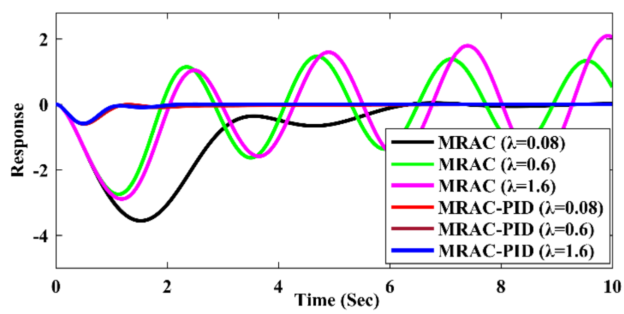

FIGURE 10. Error (reference model and plant) curve of MRAC, and MRAC-PID at different adaptation gains.

Table 4 contains the comparison of the MRAC and MRAC-PID control mechanisms for different adaptive parameters. It is noticed that the proposed MRAC-PID

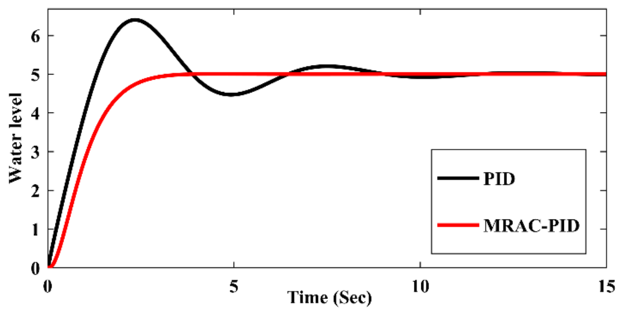

FIGURE 11. PID and proposed MRAC-PID response for increased gain.

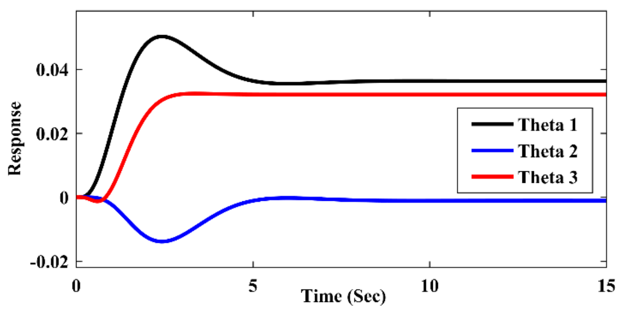

FIGURE 12. Variation of adaptive parameters (θ_1, θ_2 and θ_3) for MRAC-PID under increased gain.

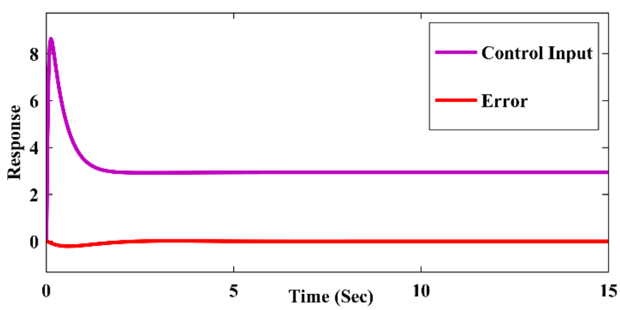

FIGURE 13. Control input and error response for MRAC-PID under increased gain.

TABLE 5. PID gain mistuning.

Controller gain	K_P	K_I	K_D
Increase	17.33	13.11	10.30
Fine-tuned	13	5	0.1
Decrease	1.2	2.0	1.50

reduces dependence as compared to MRAC, and the system exhibits robustness to maintain synchronization with the reference model by making a slight adjustment to the adaptive parameter.

If the adaptation gain is changed in a range from 0.08 to 1.6, then according to equations (35), (36), and (37), it modified the control parameters value. As they are changed with the

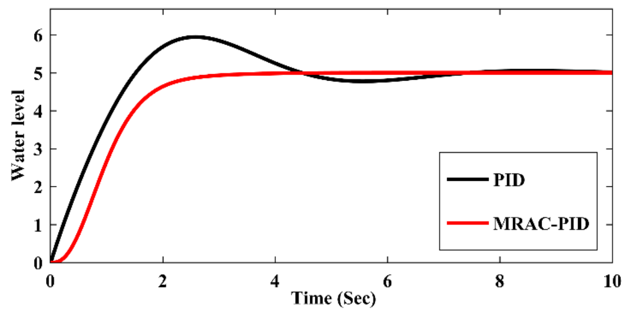

FIGURE 14. PID and proposed MRAC-PID response for decreased gain.

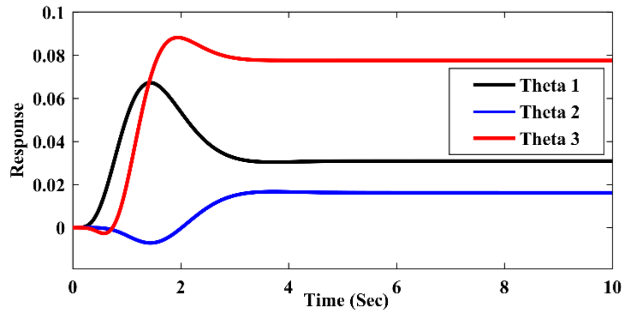

FIGURE 15. Variation of adaptive parameters (θ_1, θ_2 and θ_3) for MRAC-PID under decreased gain.

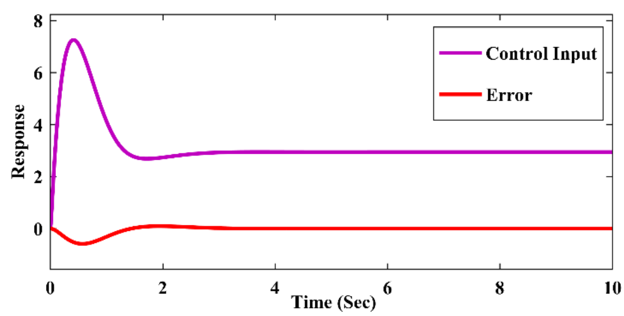

FIGURE 16. Control input and error response for MRAC-PID under decreased gain.

changing of adaption gain, the control law (u_p) also changes. The controller performance for MRAC and MRAC-PID at different adaptation gains are illustrated in Figure 9. The controller output forces the plant to follow the reference model. The error response for MRAC and MRAC-PID at different adaptation gains are shown in Figure 10. The error is reduced with the lower value of adaption gain. It implies that by MRAC and MRAC-PID with $\lambda = 0.08$, the plant output is following the desired output, which was the primary objective of the control action. Therefore, the MRAC-PID controller performs outstanding with a value of $\lambda = 0.08$.

B. PROBABILISTIC BI-LEVEL ASSESSMENT

The surrounding environment and changing operating conditions have an impact on the two tank interacting systems, introducing some unpredictable aspects that may be related

TABLE 6. Comparison of control mechanism under increased gain.

Control mechanism	Settling time (Sec)	Overshoot (%)	Rise time (Sec)	Error indices		
				IAE	ISE	ITAE
PID	11.474	27.564	1.038	0.01032	0.0001064	0.1548
MRAC-PID	3.454	0	1.601	2.312×10^{-6}	5.344×10^{-12}	3.467×10^{-5}

to modeling, tracking, disturbance, and system behavior. The probabilistic bi-level assessment is carried out by taking into consideration all such uncertainties such as gain mistuning, and dynamic system behavior.

1) LEVEL I ASSESSMENT: GAIN MISTUNING

A mistuned controller gain is the most frequent problem in control theory. Certain components of the plant's dynamics are being overpassed when adjusting the controller. Therefore, it is crucial to examine the way system responds when the controller gain is mistuned. Gain mistuning can be implemented in three ways such as fine-tuned, increase and decrease gain. The value of K_P, K_I and K_D for the increase, fine-tuned, and decrease PID gains are given in Table 5. In all cases, the λ is set at 0.08.

The PID gains are mistuned to increase their values from the fine-tuned as specified in Table 5. The response of PID and MRAC-PID under increased gain for two tank interacting systems is depicted in Figure 11. It can be seen that the proposed controller is able to follow the desired set point when the gains are mistuned. In addition, there is no oscillation in the response when the set point is being tracked. Whereas, the PID controller produces a system output that oscillates and does not precisely track the set point. The PID and MRAC-PID control mechanism takes 11.474 Sec and 3.454 Sec correspondingly to settle the desired set point.

The change of adaptive parameters (θ_1, θ_2 and θ_3) for MRAC-PID at $\lambda = 0.08$ is displayed in Figure 12. It is noticed that there is a small change in θ, and the system is able to keep up with the reference model. The control input and error response of MRAC-PID is displayed in Figure 13. The control input pushes the output of the system to follow the reference model. It is concluded that the proposed controller perfectly applied the control input to the plant so that it follows the reference model and the error becomes zero. Table 6 indicates the comparison of the control mechanism under increased gain, and it is evident that the proposed MRAC-PID strategy is supreme in all the performance indices.

For decreased gain, the response of the PID and proposed MRAC-PID is illustrated in Figure 14. The change of adaptive parameters (θ_1, θ_2 and θ_3) for MRAC-PID at $\lambda = 0.08$ is displayed in Figure 15. The control input and error response of the MRAC-PID is depicted in Figure 16.

Table 7 incorporates the detailed comparison of PID and proposed MRAC-PID control mechanism under decrease gain w.r.t settling duration, overshoot, rise time, and error rates. The PID takes 8.466 Sec, and the proposed MRAC-PID requires only 3.345 Sec to track the preferred outcome under decreased gain. The PID has a higher overshoot whereas the proposed MRAC-PID has zero overshoot. Also, the calculated error of the MRAC-PID is significantly less in contrast to the PID controller.

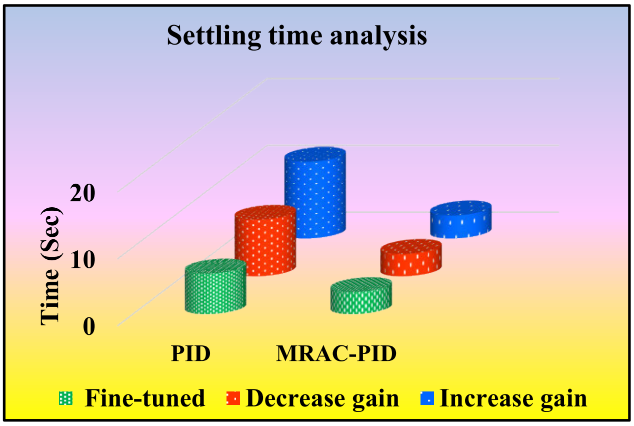

FIGURE 17. Comparative analysis under gain mistuning.

TABLE 7. Comparison of control mechanism under decreased gain.

Control mechanism	Settling time (Sec)	Overshoot (%)	Rise time (Sec)	Error indices		
				IAE	ISE	ITAE
PID	8.466	18.452	1.163	0.01343	0.0001804	0.1343
MRAC-PID	3.345	0	1.703	6.27×10^{-8}	3.93×10^{-15}	6.27×10^{-7}

TABLE 8. Comparison of control mechanism under gain mistuning.

Control mechanism	Settling time (Sec)		
	Decrease gain	Fine-tuned	Increase gain
PID	8.466	6.07	11.474
MRAC-PID	3.345	3.30	3.454

Table 8 includes the comparison of the control mechanism under gain mistuning in terms of settling time. It is determined by gain mistuning that PID performance suffers as the controller gain mistuned, but the suggested MRAC-PID consistently provides improved performance.

For the two-tank interacting system, the proposed control mechanism also ensures a quick convergence time, irrespective of gain mistuning. Figure 17 presents the infographic settling time representation of the PID and MRAC-PID under gain mistuning. As a consequence, compared to PID, the suggested MRAC-PID technique is more adaptable and fit for the two-tank interaction system.

2) LEVEL II ASSESSMENT: DYNAMIC SYSTEM BEHAVIOR

The reality is due to dynamic system behavior, modeling uncertainty, disruptions, and time-varying parameters, it is not always possible to attain desired system performance. In section V-A, a simulation with two tank interacting system parameters (System I) is carried out, and Table 1 lists its specifications. Table 9 details the parameters of system II, which is used for assessing the proposed controller's robustness as modifications are made to the system dynamics.

TABLE 9. Dynamic two-tank interacting system.

Symbol	Description	System I	System II
R_1	Resistance	1.5 Ω	1478.57 Ω
R_2	Resistance	1.7 Ω	642.86 Ω
D	Diameter of tank	92 cm	92 cm
q_{in}	Initial flow	20 lph	305 lph
τ_1	Time constant	0.9	21.42
τ_2	Time constant	1.02	9.31

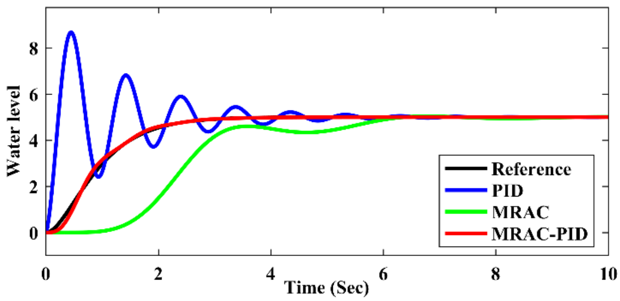

FIGURE 18. Response of the control mechanism under a dynamic two-tank interacting system (System II).

TABLE 10. Comparison of the control mechanism under dynamic two-tank interacting system (System I and System II).

Dynamic two-tank interacting system						
System	System I $G_{p1} = \frac{1.7}{0.918s^2 + 1.935s + 1}$			System II $G_{p2} = \frac{642.86}{199.42s^2 + 40.04s + 1}$		
Controller	PID	MRAC	MRAC-PID	PID	MRAC	MRAC-PID
Settling time (Sec)	6.07	6.26	3.30	9.224	7.221	3.332
Overshoot (%)	53.077	-	-	74.561	-	-
Rise time (Sec)	0.247	1.747	1.614	0.164	1.774	1.418
Performance Indices						
IAE	0.001955	0.0002056	0.0008052	0.0004458	0.01419	0.0001563
ISE	3.821×10^{-6}	0.04134	6.484×10^{-7}	1.987×10^{-7}	0.0002015	2.442×10^{-8}
ITAE	0.01955	0.1434	0.008052	0.004458	0.1419	0.001563

In this case, the PID is fine-tuned for the step input and the adaptation gain is fixed at 0.08. The response of the PID, MRAC, and MRAC-PID for the two-tank interaction system II is depicted in Figure 18. The MRAC and PID control mechanism requires 7.221 Sec and 9.224 Sec, correspondingly, although the suggested controller follows the standard model in 3.332 Sec. The two-tank interacting system under dynamic system behavior (System I and System II) is thoroughly analyzed in Table 10.

The proposed MRAC-PID control mechanism adapts to the modified system dynamics in only 3.332 Sec with negligible error while the PID's efficacy is reduced such that it takes 9.224 Sec to get the intended outcome with a considerable extent of error after modifying the system dynamics (System II). According to Table 10, the proposed mechanism has minimal overshoot and oscillations, whereas the PID controller has oscillations that are both significant and have an overshoot of approximately 74.56%. As a result, the suggested MRAC-PID technique is more flexible and appropriate for the implementation of a dynamic two-tank interacting system.

VI. CONCLUSION

In this paper, the expansion of MRAC from first to second order system is performed, and a modified version of MRAC, known as MRAC-PID, is developed. The design and analysis of the second-order conventional and modified MRAC system are undertaken. Based on the results, it is observed that the implementation of the second-order MRAC technique enables the system to effectively track the reference model. The desired response is achieved by carefully choosing a reference model that satisfies the specified system necessity. The proposed MRAC-PID has many benefits over MRAC and PID, including improved performance, quick tracking, and resilient nature. It also has negligible error functions (IAE, ISE, and ITAE). The probabilistic bi-level uncertainty framework is devised and implemented for two-tank interacting systems such as gain mistuning and dynamic system behavior. Gain mistuning is accomplished in three ways such as fine-tuned, increase and decrease gain. In the increased gain, the PID takes 11.474 Sec whereas the proposed MRAC-PID needs only 3.454 Sec to track the desired set point. In the decreased gain, the PID takes 8.466 Sec whereas the proposed MRAC-PID requires only 3.345 Sec to pursue the desired set point. Under dynamic system behavior, the proposed MRAC-PID adapts to the new dynamics in just 3.332 Sec having negligible error. The MRAC-PID requires small adjustments to be applied and minimizes dependency on adaptive gains and parameters. The recommended MRAC-PID controller is more adaptable and improved the performance of the two-tank interacting system.

REFERENCES

[1] M. Devaerakkam, K. N. Raghavan, G. K. Prince, M. J. K. Alphonse, S. Annadurai, and H. Ramachandran, "Ascendancy of level in nonlinear tank system by neuro controller," *Results Control Optim.*, vol. 12, Sep. 2023, Art. no. 100260, doi: 10.1016/j.rico.2023.100260.

[2] M. Huo, H. Luo, X. Wang, Z. Yang, and O. Kaynak, "Real-time implementation of plug-and-play process monitoring and control on an experimental three-tank system," *IEEE Trans. Ind. Informat.*, vol. 17, no. 9, pp. 6448–6456, Sep. 2021, doi: 10.1109/tii.2020.3030812.

[3] T. Xu, H. Yu, J. Yu, and X. Meng, "Adaptive disturbance attenuation control of two tank liquid level system with uncertain parameters based on port-controlled Hamiltonian," *IEEE Access*, vol. 8, pp. 47384–47392, 2020, doi: 10.1109/access.2020.2979352.

[4] E. B. Priyanka, C. Maheswari, and B. Meenakshipriya, "Parameter monitoring and control during petrol transportation using PLC based PID controller," *J. Appl. Res. Technol.*, vol. 14, no. 2, pp. 125–131, Apr. 2016, doi: 10.1016/j.jart.2016.03.004.

[5] E. Priyanka, C. Maheswari, M. Ponnibala, and S. Thangavel, "SCADA based remote monitoring and control of pressure & flow in fluid transport system using IMC-PID controller," *ASSA*, vol. 19, no. 3, pp. 140–162, Oct. 2019.

[6] E. B. Priyanka, C. Maheswari, and S. Thangavel, "Online monitoring and control of flow rate in oil pipelines transportation system by using PLC based fuzzy-PID controller," *Flow Meas. Instrum.*, vol. 62, pp. 144–151, Aug. 2018, doi: 10.1016/j.flowmeasinst.2018.02.010.

[7] K. S. Rao, V. B. Kumar, V. N. S. Praneeth, and Y. V. P. Kumar, "Fuzzy logic theory-based pi controller tuning for improved control of liquid level system," in *Intelligent Algorithms for Analysis and Control of Dynamical Systems*. New York, NY, USA: Springer, Nov. 2020, pp. 133–143, doi: 10.1007/978-981-15-8045-1_14.

[8] A. Fakhrazari and M. Boroushaki, "Adaptive critic-based neurofuzzy controller for the steam generator water level," *IEEE Trans. Nucl. Sci.*, vol. 55, no. 3, pp. 1678–1685, Jun. 2008, doi: 10.1109/TNS.2008.924058.

[9] L. Wei, F. Fang, and Y. Shi, "Adaptive backstepping-based composite nonlinear feedback water level control for the nuclear U-tube steam generator," *IEEE Trans. Control Syst. Technol.*, vol. 22, no. 1, pp. 369–377, Jan. 2014.

[10] A. Noordin, M. A. M. Basri, Z. Mohamed, and I. M. Lazim, "Adaptive PID controller using sliding mode control approaches for quadrotor UAV attitude and position stabilization," *Arabian J. Sci. Eng.*, vol. 46, no. 2, pp. 963–981, Jul. 2020, doi: 10.1007/s13369-020-04742-w.

[11] J. Espín, F. Castrillon, H. Leiva, and O. Camacho, "A modified Smith predictor based–sliding mode control approach for integrating processes with dead time," *Alexandria Eng. J.*, vol. 61, no. 12, pp. 10119–10137, Dec. 2022, doi: 10.1016/j.aej.2022.03.045.

[12] D. Castellanos-Cárdenas, F. Castrillón, R. E. Vásquez, N. L. Posada, and O. Camacho, "A new sliding mode control tuning approach for second-order inverse-response plus variable dead time processes," *J. Process Control*, vol. 115, pp. 77–88, Jul. 2022, doi: 10.1016/j.jprocont.2022.05.001.

[13] S. Sutha, P. Lakshmi, and S. Sankaranarayanan, "Fractional-order sliding mode controller design for a modified quadruple tank process via multi-level switching," *Comput. Electr. Eng.*, vol. 45, pp. 10–21, Jul. 2015.

[14] B. Kar and P. Roy, "A comparative study between cascaded FOPI–FOPD and IOPI–IOPD controllers applied to a level control problem in a coupled tank system," *J. Control, Autom. Electr. Syst.*, vol. 29, no. 3, pp. 340–349, Jun. 2018.

[15] D. Acharya and D. K. Das, "Swarm optimization approach to design PID controller for artificially ventilated human respiratory system," *Comput. Methods Programs Biomed.*, vol. 198, Jan. 2021, Art. no. 105776, doi: 10.1016/j.cmpb.2020.105776.

[16] J. Pongfai, C. Angeli, P. Shi, X. Su, and W. Assawinchaichote, "Optimal PID controller autotuning design for MIMO nonlinear systems based on the adaptive SLP algorithm," *Int. J. Control, Autom. Syst.*, vol. 19, no. 1, pp. 392–403, Sep. 2020, doi: 10.1007/s12555-019-0680-6.

[17] W. Zeng, Q. Jiang, J. Xie, and T. Yu, "A fuzzy-PID composite controller for core power control of liquid molten salt reactor," *Ann. Nucl. Energy*, vol. 139, May 2020, Art. no. 107234, doi: 10.1016/j.anucene.2019.107234.

[18] R. Arivalahan, P. Tamilarasan, and M. Kamalakannan, "Liquid level control in two tanks spherical interacting system with fractional order proportional integral derivative controller using hybrid technique: A hybrid technique," *Adv. Eng. Softw.*, vol. 175, Jan. 2023, Art. no. 103316, doi: 10.1016/j.advengsoft.2022.103316.

[19] A. Jegatheesh and C. Agees Kumar, "Novel fuzzy fractional order PID controller for non linear interacting coupled spherical tank system for level process," *Microprocessors Microsystems*, vol. 72, Feb. 2020, Art. no. 102948, doi: 10.1016/j.micpro.2019.102948.

[20] G. Maruthi Prasad and A. Seshagiri Rao, "Evaluation of gap-metric based multi-model control schemes for nonlinear systems: An experimental study," *ISA Trans.*, vol. 94, pp. 246–254, Nov. 2019, doi: 10.1016/j.isatra.2019.04.006.

[21] H. Gouta, S. Hadj Saïd, A. Turki, and F. M'Sahli, "Experimental sensorless control for a coupled two-tank system using high gain adaptive observer and nonlinear generalized predictive strategy," *ISA Trans.*, vol. 87, pp. 187–199, Apr. 2019, doi: 10.1016/j.isatra.2018.11.046.

[22] N. Divya, S. Manoharan, J. Arulvadivu, and P. Palpandian, "An efficient tuning of fractional order PID controller for an industrial control process," *Mater. Today, Proc.*, vol. 57, pp. 1654–1659, 2022, doi: 10.1016/j.matpr.2021.12.255.

[23] J. Espín, S. Estrada, D. Benítez, and O. Camacho, "A hybrid sliding mode controller approach for level control in the nuclear power plant steam generators," *Alexandria Eng. J.*, vol. 64, pp. 627–644, Feb. 2023, doi: 10.1016/j.aej.2022.08.046.

[24] C. Pu, J. Ren, and J. Su, "The sliding mode control of the drum water level based on extended state observer," *IEEE Access*, vol. 7, pp. 135942–135948, 2019, doi: 10.1109/access.2019.2940056.

[25] E. B. Priyanka, C. Maheswari, S. Thangavel, and M. P. Bala, "Integrating IoT with LQR-PID controller for online surveillance and control of flow and pressure in fluid transportation system," *J. Ind. Inf. Integr.*, vol. 17, Mar. 2020, Art. no. 100127, doi: 10.1016/j.jii.2020.100127.

[26] Y. Xu, K. Zhao, P. Guo, W. Jiang, X. Wu, and W. Sun, "Design of type-2 fuzzy fractional-order proportional-integral-derivative controller and multi-objective parameter optimization under load reduction condition of the pumped storage unit," *J. Energy Storage*, vol. 50, Jun. 2022, Art. no. 104227, doi: 10.1016/j.est.2022.104227.

[27] G. K. E. and A. J., "Control of nonlinear two-tank hybrid system using sliding mode controller with fractional-order PI-D sliding surface," *Comput. Electr. Eng.*, vol. 71, pp. 953–965, Oct. 2018, doi: 10.1016/j.compeleceng.2017.10.005.

[28] Z. Xu, Q. Fan, and J. Zhao, "Gain-scheduled equivalent-cascade IMC tuning method for water level control system of nuclear steam generator," *Processes*, vol. 8, no. 9, p. 1160, Sep. 2020, doi: 10.3390/pr8091160.

[29] M. Herrera, O. Camacho, H. Leiva, and C. Smith, "An approach of dynamic sliding mode control for chemical processes," *J. Process Control*, vol. 85, pp. 112–120, Jan. 2020, doi: 10.1016/j.jprocont.2019.11.008.

[30] Y. Sun, H. Qiang, L. Wang, W. Ji, and A. Mardani, "A fuzzy-logic-system-based cooperative control for the multielectromagnets suspension system of Maglev trains with experimental verification," *IEEE Trans. Fuzzy Syst.*, vol. 31, no. 10, pp. 3411–3422, Oct. 2023, doi: 10.1109/TFUZZ.2023.3257036.

[31] Y. Sun, J. Xu, G. Lin, and N. Sun, "Adaptive neural network control for Maglev vehicle systems with time-varying mass and external disturbance," *Neural Comput. Appl.*, vol. 35, no. 17, pp. 12361–12372, Mar. 2021, doi: 10.1007/s00521-021-05874-2.

[32] Ishwarya, Janakiraman, S. Sekar, and T. G. Vaishali, "Design of model reference adaptive controller for cylinder tank system," *Int. J. Pure Appl. Math.*, vol. 118, no. 20, pp. 2007–2013, 2018.

[33] S. Manna, D. K. Singh, and A. K. Akella, "Design and implementation of MRAC & MRAC-PID feedback for turntable," *Gazi Univ. J. Sci.*, vol. 36, no. 3, pp. 1171–1185, Sep. 2023, doi: 10.35378/gujs.1052850.

[34] K. J. Astrom and B. Wittenmark, *Adaptive Control*, 2nd ed. Mineola, NY, USA: Dover, 2001, pp. 185–225.

SAIBAL MANNA received the M.Tech. degree in control and automation from VIT, Vellore, India, in 2019. He submitted the Ph.D. thesis with the Department of Electrical Engineering, National Institute of Technology, Jamshedpur, India, in June 2023. He is currently an Assistant Professor with the Department of Electrical and Electronics Engineering, ABES Engineering College, Ghaziabad, Uttar Pradesh, India. His research interests include adaptive control, optimal control, PV, renewable energy, active suspension systems, MPPT, EV, microgrid, and modern control systems.

DEEPAK KUMAR SINGH was born in Dehri, Bihar, India. He received the M.Tech. degree in control system from BIT Sindri, Dhanbad, India, in 2019. He is currently pursuing the Ph.D. degree with the Department of Electrical Engineering, National Institute of Technology, Jamshedpur, India. His areas of research interests include solar power estimation, modeling and control of renewable energy resources, and modern control applications.

YAZEED YASIN GHADI received the Ph.D. degree in electrical and computer engineering from Queensland University. He was a Postdoctoral Researcher with Queensland University, before joining Al Ain University. He is currently an Assistant Professor of software engineering with Al Ain University. He has published more than 25 peer-reviewed journals and conference papers and holds three pending patents. His current research interests include developing novel electro-acoustic-optic neural interfaces for large-scale high-resolution electrophysiology and distributed optogenetic stimulation. He was a recipient of several awards. His dissertation on developing novel hybrid plasmonic photonic on-chip biochemical sensors received the Sigma Xi Best Ph.D. Thesis Award.

AMR YOUSEF received the B.Sc. degree from the Engineering Mathematics Department, Alexandria University, in 2001, and the M.Sc. degree from the Electrical Engineering Department, Alexandria University, in 2006, and the Ph.D. degree in electrical and computer engineering from Old Dominion University (ODU), in May 2012. He is an Assistant Professor with the Electrical Engineering Department, University of Business and Technology, Saudi Arabia. He was a Postdoctoral Research Associate with the Old Dominion Vision Laboratory, USA. His research interests include optimization techniques, image processing/computer vision, and machine learning algorithms. He is a member of SPIE and OSA.

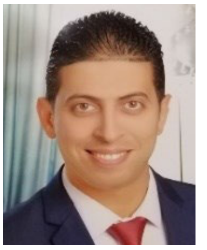

HOSSAM KOTB received the B.Sc., M.Sc., and Ph.D. degrees in electrical engineering from the Faculty of Engineering, Alexandria University, Alexandria, Egypt, in 2009, 2013, and 2020, respectively. His Ph.D. research work was focused on the performance enhancement of renewable energy conversion systems. Currently, he is an Assistant Professor with the Electrical Power and Machines Department, Faculty of Engineering, Alexandria University. His research interests include power system analysis, electrical drives, modern control techniques, smart grids, optimization, electric vehicles, and renewable energy systems. He is an Associate Editor of *Alexandria Engineering Journal* (AEJ).

KAREEM M. ABORAS received the B.Sc., M.Sc., and Ph.D. degrees in electrical engineering from the Faculty of Engineering, Alexandria University, Alexandria, Egypt, in 2010, 2015, and 2019, respectively. His Ph.D. research work was focused on the performance enhancement of renewable energy conversion systems. Currently, he is an Assistant Professor with the Electrical Power and Machines Department, Faculty of Engineering, Alexandria University. His research interests include power electronics, control, drives, power systems, smart grids, microgrids, power quality, optimizations, electric vehicles, machine learning, modeling, fuel cells, HVDC, and renewable energy systems. He is a Reviewer of IEEE TRANSACTIONS ON ENERGY CONVERSION, *Electric Power Systems Research*, *Smart Science*, *Alexandria Engineering Journal*, IET, *Energy Reports*, IEEE ACCESS, *Cybernetics and Systems*, *Protection and Control of Modern Power Systems*, MDPI, *Journal of Advanced Research in Applied Sciences and Engineering Technology*, *Cogent Engineering*, and Hindawi journals.